

# Millimeter-wave modulated optical pulse generated by pulse repetition rate multiplication and temporal Talbot effect

Zhengqing Pan (潘政清), Qing Ye (叶青), Haiwen Cai (蔡海文),  
Ronghui Qu (瞿荣辉), and Zujie Fang (方祖捷)

Shanghai Institute of Optics and Fine Mechanics, Chinese Academy of Sciences, Shanghai 201800

Received February 18, 2008

A novel scheme was proposed to generate a millimeter-wave (MMW) optical pulse by combining pulse repetition rate multiplication (PRRM) technology and temporal Talbot effect (TTE). A cascaded Mach-Zehnder interferometer (MZI) lattice was used for PRRM, and a linearly chirped fiber grating (LCFG) was used as TTE. The basic principle was analyzed by using a Gaussian input short pulse and its characteristics were discussed by numerical simulation. It is shown that the proposed scheme is feasible for MMW signal generation and has potential merits for practical application of radio over fiber (ROF) technology.

OCIS codes: 060.2330, 060.2630, 060.4080, 060.1810.

doi: 10.3788/COL20080609.0634.

In recent years, radio over fiber (ROF), which is expected to be used in future mobile communication and advanced microwave technologies, has attracted great attention. Generation of millimeter-wave (MMW) signals is one of the key problems to be solved in transmitter of ROF systems. To overcome the electronic bottleneck, photonic assisted methods have been paid more attention, such as heterodyne method, which uses beating between two light waves with frequency difference corresponding to the required microwave frequency<sup>[1]</sup>. Another attractive method is schemes by using passive devices, such as direct space-time pulse shaper<sup>[2]</sup>, which separates different frequency composition of the input optical pulse, adjusts their amplitudes and phases, and then recombines them to generate a microwave modulated optical pulse. A specially designed superstructure fiber Bragg grating can also generate self beating within an optical pulse<sup>[3]</sup>. However, there are still some problems to be solved in passive device-based methods, one of which is the low energy efficiency. Temporal Talbot effect (TTE), which is caused by interferences between the identical pulse trains traveling in the dispersive medium, is used to multiply the repetition rate of a periodic pulse sequence<sup>[4,5]</sup>, and is proposed to generate microwave modulated optical signals<sup>[6,7]</sup>. New schemes by using different mechanisms are still to be investigated.

In this letter, a novel scheme combining TTE and passive pulse repetition rate multiplication (PRRM) was proposed to realize MMW modulated optical pulse signal generation. The passive PRRM consists of a fiber Mach-Zehnder interferometer (MZI) lattice<sup>[8]</sup>, which transforms a single optical pulse to a  $N$ -pulse train with a relatively wide interval. A linearly chirped fiber grating (LCFG) is used as a dispersive component in which TTE occurs. The pulse interval is further reduced to transform the pulse train into a high frequency modulated signal. The basic characteristics of microwave modulated optical signal generated by PRRM and TTE are analyzed theoretically, and its advantages and technological issues are discussed. It is shown that the new scheme is feasible and suitable for some applications.

A schematic diagram of our proposal is shown in Fig. 1. Firstly, a single optical pulse is transformed into a  $N$ -pulse train by a cascaded MZI. The path difference  $\Delta L$  of each MZI is designed to change with its stage number  $i$  as  $\Delta L_i = \Delta L_1/2^{i-1}$  ( $i = 1 \cdots k$ ), if  $k$  stages of MZI are used. A simple calculation gives that  $N = 2^k$ , and the interval between the pulses in the generated train is  $T_1 = (n\Delta L_1/c)/2^{k-1}$ , where  $n$  is the index and  $c$  is the light velocity in vacuum. Then, ideally, the impulse response function of the PRRM can be written as<sup>[8]</sup>

$$h_1(t) = \sum_{p=0}^{N-1} a(t)\delta(t - pT_1), \quad (1)$$

where  $a(t)$  is the envelope of pulse sequence which depends mainly on splitting ratios of the couplers, and will be a constant if ideal 3-dB couplers used;  $\delta(t)$  is the delta function,  $p$  is the sequence number in the pulse train. Consequently, the repetition rate of the pulse train is  $f_1 = 1/T_1 = 2^{k-1}c/(n\Delta L_1)$ .

The second part of the proposed scheme plays a role of TTE, which consists of a circulator and a LCFG designed with a constant first-order dispersion coefficient defined as  $\Phi'' = \partial^2\Phi/\partial\omega^2$ , where  $\Phi$  is the phase shift of light wave passing through the LCFG, and the corresponding impulse response function is<sup>[9-11]</sup>

$$h_2(t) = \frac{i}{\sqrt{i2\pi\Phi''}} \exp \frac{-it^2}{2\Phi''}. \quad (2)$$

Each pulse in the train will suffer changes in its phase when passing through the LCFG, and the pulse waveform will be broadened. They will interfere with each other,

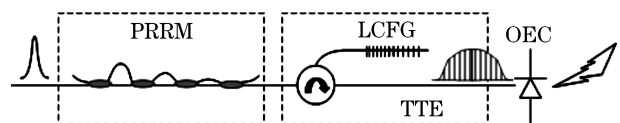


Fig. 1. Schematic for MMW modulated optical signal generation. OEC: optical to electrical connection.

resulting in self-imaging in time domain under certain conditions, i.e., TTE. The combined impulse response function  $h(t)$  can be obtained by a convolution integral of  $h_1(t)$  and  $h_2(t)$  as

$$\begin{aligned} h(t) &= h_1(t) \otimes h_2(t) \\ &= \frac{i}{\sqrt{i2\pi\Phi''}} \sum_{p=0}^{N-1} a(pT_1) \exp \frac{-i(t-pT_1)^2}{2\Phi''}. \end{aligned} \quad (3)$$

According to the analysis of TTE<sup>[4]</sup>, the dispersion required for multiplying the repetition rate of incident pulse train by a factor of  $M$  should satisfy the Talbot condition:

$$|\Phi''| = \frac{T_1^2}{2\pi M}. \quad (4)$$

Under this condition, the modulation rate will then be increased to  $f_2 = Mf_1$ .

As a typical example, a transform-limited Gaussian pulse can be taken as an input pulse with a waveform of  $E_{\text{in}} = E_0 \exp(-t^2/2\tau^2)$ , where  $E_0$  and  $\tau$  are the amplitude and the root-mean-square (RMS) width. The output pulse can be obtained by convolution integral:

$$\begin{aligned} E_{\text{out}} &= E_{\text{in}} \otimes h(t) \\ &= E_0 \sum_{p=0}^{N-1} \frac{a(pT_1)}{\sqrt{1-i\Phi''/\tau^2}} \exp \frac{-(t-pT_1)^2}{2(\tau^2-i\Phi'')} \\ &\approx E_0 \tau \sqrt{\frac{i}{\Phi''}} \sum_{p=0}^{N-1} a(pT_1) \exp \frac{-(t-pT_1)^2 \tau^2}{2\Phi''^2} \\ &\quad \times \exp \frac{-i(t-pT_1)^2}{2\Phi''}. \end{aligned} \quad (5)$$

The last approximate equality is for the case that the input pulse is short enough to satisfy the condition of  $\tau^2 \ll \Phi''$ . The intensity of the output can be deduced by  $I_{\text{out}} = |E_{\text{out}}|^2$ , in which the interference between pulses will produce a phase factor proportional to a term as follows:

$$\begin{aligned} &\cos \left[ \frac{(t-pT_1)^2}{2\Phi''} - \frac{(t-p'T_1)^2}{2\Phi''} \right] \\ &= \cos \left[ \frac{(p-p')tT_1}{\Phi''} + \frac{(p^2-p'^2)T_1^2}{2\Phi''} \right], \end{aligned} \quad (6)$$

where  $p, p' = 0 \dots (N-1)$ , which contains a vibration term with frequency of  $(p-p')T_1/2\pi\Phi''$ ; the fundamental modulation frequency is  $f_2 = T_1/(2\pi\Phi'') = M/T_1 = Mf_1$  from the interference between adjacent pulses with  $p-p' = 1$ . If the Talbot condition Eq. (4) is satisfied, the second term in the right part of Eq. (6) can be reduced to an integer multiple of  $\pi$ . Therefore, the intensity of output can be written as

$$I_{\text{out}} = I_0 + I_1 \cos(T_1/\Phi'')t + I_2 \cos(2T_1/\Phi'')t + \dots \quad (7)$$

The first three terms are concerned mostly, which can be deduced from Eq. (5) as follows:

$$\begin{aligned} I_0 &= 2E_0^2 \nu \tau \exp(-\nu^2 t^2) \sum_{m=1}^{N/2} \exp \frac{-(2m-1)^2 \nu^2 T_1^2}{4} \\ &\quad \times \cosh[(2m-1)\nu^2 T_1 t], \end{aligned} \quad (8a)$$

$$\begin{aligned} I_1 &= 2E_0^2 \nu \tau \exp(-\nu^2 t^2) \exp \frac{-\nu^2 T_1^2}{4} \\ &\quad \times [1 + 2 \sum_{m=1}^{N/2-1} \exp(-m^2 \nu^2 T_1^2) \cosh(2m\nu^2 T_1 t)], \end{aligned} \quad (8b)$$

$$\begin{aligned} I_2 &= 4E_0^2 \nu \tau \exp[-\nu^2(t^2 + T_1^2)] \\ &\quad \times \sum_{m=0}^{N/2-2} \exp[-(m + \frac{1}{2})^2 \nu^2 T_1^2] \cosh[(2m+1)\nu^2 T_1 t], \end{aligned} \quad (8c)$$

where the original  $t$  is moved to the middle point of the output, as  $t \rightarrow t - (N-1)T_1/2$ , and  $\nu = \tau/|\Phi''|$  is used. It is shown that the waveforms are composed of a Gaussian function and one or more hyperbolic cosine functions; the extinction ratio of the RF oscillation will be near 100% at the center, while at the two wings will be reduced due to the hyperbolic pedestal, which is higher for larger input pulse width  $\tau$ . In addition, the amplitudes of bands for  $2f_2$  or higher will be much smaller than the fundamental  $f_2$  band.

Equations (1)–(8) give the basic quantitative relations among the parameters in the PRRM+TTE scheme. The scheme includes two stages to multiplex the repetition rates. The modulation frequency depends on the repetition rate multiplication  $N$  at PRRM and  $M$  at the TTE stage, which are determined mainly by the dispersion of LCFG. The input pulse width will not only affect the resulted frequency, but also will influence the output waveform performances. The MZI lattice is simple and low cost, and the TTE has potentials for much higher frequency pulse duplicating. The above basic analysis shows that the scheme is feasible for generation of high-frequency modulated optical signals under properly designed parameters.

To demonstrate the performance of the proposed scheme, numerical simulation results based on the above theoretical expressions are given for the target radio frequency (RF) of 60 GHz. Impact of input pulse width is investigated for  $N = 4$  and  $T_1 = 200$  ps, which means the multiplication at TTF stage has to be set at  $M = 12$ , and the dispersion of the LCFG is set to be  $\Phi'' = 530$  ps<sup>2</sup>. Meanwhile, the number of cascaded MZI is  $k = 2$ , and the path difference of the first MZI is set as  $n\Delta L \approx 60$  mm. RF waveforms are calculated for input Gaussian pulse widths of  $\tau = 2, 4, \text{ and } 6$  ps, as shown in Fig. 2, respectively. It is noticed that the modulation depth of the output pulse is quite large in the middle part of envelop, but there are obvious pedestals with heights depending greatly on the input pulse width at its two wings as described by Eqs. (8a)–(8c). Obviously, it is due to the

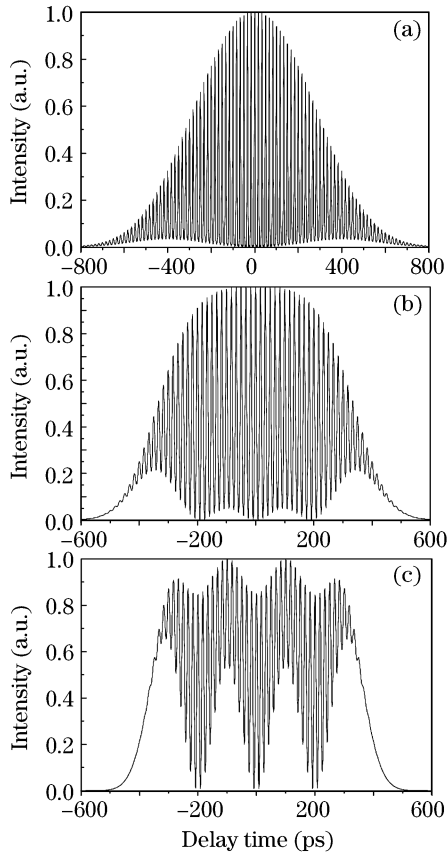


Fig. 2. Output waveforms for input pulse width of (a) 2 ps, (b) 4 ps, and (c) 6 ps with  $N = 4$ .

multiplication mechanism of PRRM and TTE, and it is necessary to use input pulse with width much shorter than the period of requested RF, which is about 17 ps here.

The effect of the pulse number at the PRRM stage is studied for  $\tau = 3$  ps,  $N = 2, 4$ , and 8 with pulse spacing of 400, 200, and 100 ps, and the correspondingly multiplication ratio  $M$  of 24, 12, and 6, respectively. It is deduced from the calculated results shown in Fig. 3 that more pulse number input to TTE will help to lower the amplitude of two wing pedestals, enhance energy efficiency, and broaden the top width of the envelop. This phenomenon can be interpreted that the more number of pulses involved in the pulse sequence for transforming, the more approximate to the ideal temporal Talbot effect<sup>[10]</sup>.

To evaluate the impact of input pulse width and pulse number at the first multiplication, a weighted average modulation depth is defined as

$$\bar{m} = \frac{\sum_i \frac{(I_{\text{peak}} - I_{\text{valley}})_i U_i}{(I_{\text{peak}} + I_{\text{valley}})_i}}{\sum_i U_i}, \quad (9)$$

where  $U_i = \int_{1/f_2} I_i(t) dt$  is the energy in  $i$ th period. Figure 4 shows calculated relations between  $\bar{m}$  and  $\tau$  for different pulse numbers of  $N$ . As expected, the modulation depth will decrease quickly with the increase of pulse width, and a wider input pulse width needs a larger pulse number  $N$  to keep the modulation depth larger. Figure 5 gives a typical RF spectrum for  $\tau = 3$  ps and

$N = 4$ , showing a main lobe of band width of about 1.8 GHz, and symmetric side lobes near  $(60 \pm 2.2)$  GHz, and so on. In the simulations, the approximation condition

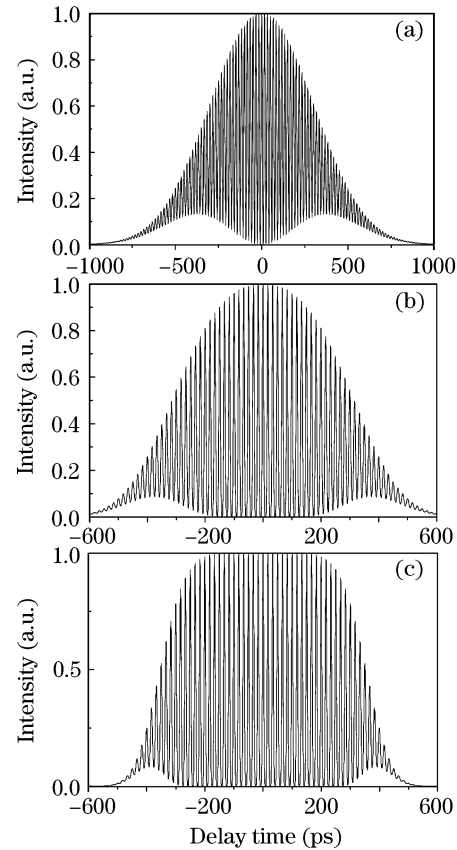


Fig. 3. Output waveforms for  $\tau = 3$  ps with (a)  $N = 2$ , (b)  $N = 4$ , and (c)  $N = 8$ .

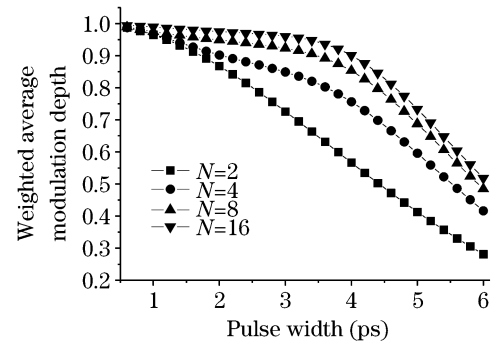


Fig. 4. Averaged modulation depth versus input pulse width.

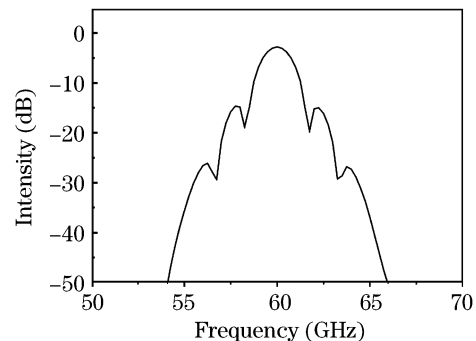


Fig. 5. A typical RF spectrum.

in Eq. (5),  $\tau^2 \ll \Phi''$ , is not taken, bringing about a minor revision to the above theoretical formulas.

As the core of TTE part, parameters of the LCFG will influence performances of the MMW generation system greatly. First of all, dispersion of the LCFG should meet the Talbot condition Eq. (4). For the same RF frequency and envelop width, Eq. (4) can be rewritten as  $\Phi'' = T_1 T_2 / (2\pi)$ . That means the dispersion should match the pulse spacing produced at MZI PRRM and the required RF wave period. Another requirement for the LCFG is that its spectral width as a reflective filter should cover the spectrum of the input pulse. For example, the spectral half width  $1/e$  maximum of the input pulse intensity for  $\tau = 3$  ps is about 1.2 nm. If a 10-cm-long LCFG with above dispersion is used, its spectral width will be 2.33 nm, which is large enough to cover the input spectrum. Such a fiber grating should be available commercially, even if for shorter input pulses.

It is necessary to investigate the influence of LCFG dispersion value on the quality of the MMW signal, because the dispersion cannot be controlled precisely in its practical fabrication. It can be deduced from Eq. (5) that if the Talbot condition is not satisfied, the interferences will have phases different from the integer multiple of  $\pi$ , and may have different values for different pairs of  $p$  and  $p'$ , which can be regarded as a phase noise to the MMW. Figure 6 shows a typical output waveform and its RF spectrum calculated for a dispersion value of 2% deviated from the ideal Talbot value. The input pulse width is 3 ps and the pulse number is  $N = 4$ . It is seen that the waveform is changed obviously, the spectrum becomes non-symmetric, and the peak RF frequency shifts a little as well.

To evaluate the influence of dispersion deviation, a cross-correlation coefficient is introduced as used in Ref. [11], which is defined as  $C = \int I_T I_D dt / [\int I_T^2 dt * \int I_D^2 dt]^{1/2}$ , where  $I_T$  and  $I_D$  are the waveforms for dispersion of Talbot condition and for a deviated one,

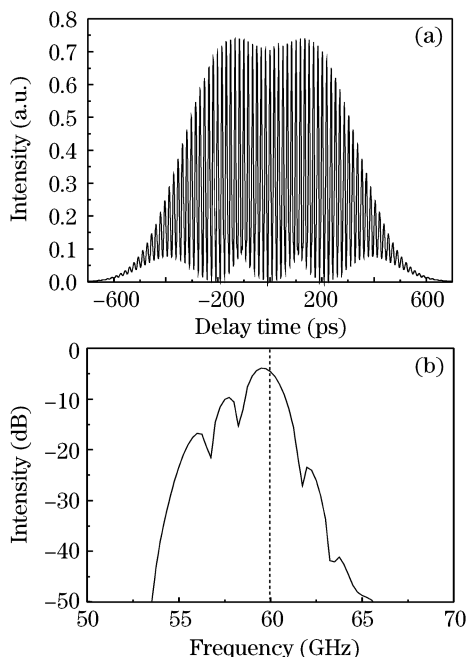


Fig. 6. (a) Optical pulse waveform and (b) RF spectrum from LCFG with 2% deviation.

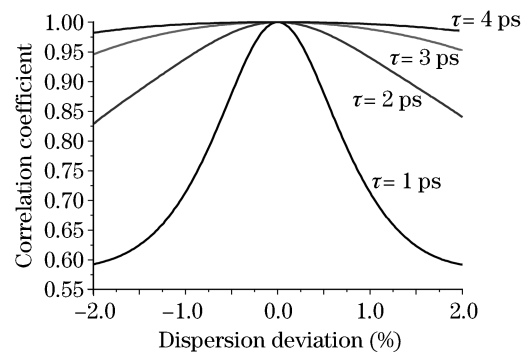


Fig. 7. Cross-correlation coefficient versus dispersion deviation.

respectively. Figure 7 shows the correlation varied with the dispersion deviation for different input pulse widths, indicating that the influence becomes critical for short pulse width. To get better performance, it is necessary to take a trade-off between the system parameters, including  $N$ ,  $T_1$ ,  $M$ , and  $\tau$ . A smaller  $\tau$  results not only in larger modulation depth, but also in stricter controlling precision requirement for a better waveform.

A passive all-fiber device, employing the passive PRRM technology and TTE, is proposed for the generation of MMW pulse signal. The passive PRRM is used as a generator of relative low frequent pulse train, and a LCFG is used to multiply the pulse train to a MMW optical pulse envelope based on TTE. The performances of the generated MMW pulse, including modulation depth, RF spectrum, and influence of parameter deviation, are analyzed in detail. Most of the components used in the system, such as LCFG, fiber or waveguide couplers, MZI, fiber circulator, and high-speed O-E converter, are reliable technologically and cost-effective. The ultra-short laser sources are being used more and more widely. The theoretical analysis and simulation results show that the proposed scheme is feasible and has a good application foreground in the area of ROF and microwave photonics.

Z. Pan's e-mail address is blitheforest@yahoo.com.

## References

1. A. C. Bordonalli, C. Walton, and A. J. Seeds, *J. Lightwave Technol.* **17**, 328 (1999).
2. J. D. McKinney, D. Seo, D. E. Leaird, and A. M. Weiner, *J. Lightwave Technol.* **21**, 3020 (2003).
3. Q. Ye, F. Liu, R. Qu, and Z. Fang, *Acta Opt. Sin.* (in Chinese) **10**, 1464 (2006).
4. I. Shake, H. Takara, S. Kawanishi, and M. Saruwatari, *Electron. Lett.* **34**, 792 (1998).
5. S. Longhi, M. Marano, P. Laporta, O. Svelto, M. Belmonte, B. Agogliati, L. Arcangeli, V. Pruneri, M. N. Zervas, and M. Ibsen, *Opt. Lett.* **25**, 1481 (2000).
6. J. Azaña, N. K. Berger, B. Levit, V. Smulakovsky, and B. Fischer, *Opt. Lett.* **29**, 2849 (2004).
7. V. Torres-Company, M. Fernández-Alonso, J. Lancis, J. C. Barreiro, and P. Andrés, *Opt. Express* **14**, 9617 (2006).
8. B. Xia and L. R. Chen, *IEEE J. Sel. Top. Quantum Electron.* **11**, 165 (2005).
9. G. P. Agrawal, *Nonlinear Fiber Optics* (3rd edn.) (Academic, Boston, 2001), Chapt.3.
10. J. Azaña, *J. Opt. Soc. Am. B* **20**, 83 (2003).
11. J. Azaña and M. A. Muriel, *Appl. Opt.* **38**, 6700 (1999).